

# Characterizing the Tick Carboxypeptidase Inhibitor MOLECULAR BASIS FOR ITS TWO-DOMAIN NATURE\*<sup>§</sup>

Received for publication, March 10, 2006, and in revised form, May 5, 2006. Published, JBC Papers in Press, June 7, 2006, DOI 10.1074/jbc.M602301200

Joan L. Arolas<sup>†1</sup>, Sílvia Bronsoms<sup>‡</sup>, Salvador Ventura<sup>‡2</sup>, Francesc X. Aviles<sup>‡3</sup>, and Juan J. Calvete<sup>§</sup>

From the <sup>†</sup>Institut de Biotecnologia i Biomedicina and Departament de Bioquímica i Biologia Molecular, Universitat Autònoma de Barcelona, 08193 Bellaterra, Barcelona and the <sup>§</sup>Instituto de Biomedicina de Valencia, Consejo Superior de Investigaciones Científicas, Jaime Roig 11, 46010 Valencia, Spain

Tick carboxypeptidase inhibitor (TCI) is a small, disulfide-rich protein that selectively inhibits metalloproteinases and strongly accelerates the fibrinolysis of blood clots. TCI consists of two domains that are structurally very similar, each containing three disulfide bonds arranged in an almost identical fashion. The oxidative folding and reductive unfolding pathways of TCI and its separated domains have been characterized by kinetic and structural analysis of the acid-trapped folding intermediates. TCI folding proceeds through a sequential formation of 1-, 2-, 3-, 4-, 5-, and 6-disulfide species to reach the native form. Folding intermediates of TCI comprise two predominant 3-disulfide species (named IIIa and IIIb) and a major 6-disulfide scrambled isomer (Xa) that consecutively accumulate along the reaction and are strongly prevented by the presence of protein disulfide isomerase. This study demonstrates that IIIa and IIIb are 3-disulfide species containing the native disulfide pairings of the N- and C-terminal domains of TCI, respectively, and explains why the two domains of TCI fold sequentially and independently. Also, we show that the reductive unfolding of TCI undergoes two main independent unfolding events through the formation of IIIa and IIIb intermediates. Together, the comparison of the folding, stability, and inhibitory activity of TCI with those of the isolated domains reveals the reasons behind the two-domain nature of this protein: both domains contribute to the specificity and high affinity of its double-headed binding to carboxypeptidases. The results obtained herein provide valuable information for the design of more potent and selective TCI molecules.

The mechanism by which an unfolded protein achieves its native state is one of the most complex problems in structural biology. Understanding the sequence of folding events in pro-

teins may not only help to predict protein structures from amino acid sequences but also provide invaluable information to a variety of related fields, such as protein design or protein misfolding associated with pathological diseases (1, 2). A number of studies concerning folding have been focused on small, disulfide-rich proteins, given that the chemistry of disulfide bond formation allows the trapping and subsequent characterization of the folding intermediates that accumulate, something difficult to attain with disulfide-free proteins (3, 4). In oxidative folding, reduced and denatured proteins are allowed to recover both its native disulfide bonds and native structures in the absence or presence of redox agents. Bovine pancreatic trypsin inhibitor, ribonuclease A, lysozyme,  $\alpha$ -lactalbumin, and hirudin have been extensively investigated using this methodology (5–9). The heterogeneity and structures of the intermediates that occur during the process define their respective folding landscapes (10).

Although most of the analyzed proteins comprise a small, single-domain fold containing three or four disulfide bonds, a great diversity of folding mechanisms is observed among them. Bovine pancreatic trypsin inhibitor-like proteins fold through a few disulfide intermediates that adopt native disulfide pairings and native-like (sub)structures (11, 12). These intermediates seem to funnel protein conformations toward the native state and prevent the accumulation of non-native disulfide (scrambled) isomers. In contrast, the folding of hirudin-like proteins (*e.g.* tick anticoagulant peptide and potato carboxypeptidase inhibitor) displays a far more heterogeneous population of intermediates (at least 20 out of 74 possible) that includes scrambled isomers (13, 14). Conversion of these latter species into the native protein usually represents the rate-limiting step of the folding reaction. Finally, other disulfide-rich proteins such as epidermal growth factor or leech carboxypeptidase inhibitor are characterized by the presence of both native-like intermediates and scrambled isomers, showing similarities to both the folding of bovine pancreatic trypsin inhibitor and hirudin (15, 16).

The tick carboxypeptidase inhibitor (TCI)<sup>4</sup> is the first metal-

\* This work was supported in part by the Ministerio de Educación y Ciencia (MEC), Spain (Grants BIO2004-05879, GEN03-20642-C09-05, and BFU2004-01432/BMC) and by the Centre de Referència en Biotecnologia (Generalitat de Catalunya, Spain). The costs of publication of this article were defrayed in part by the payment of page charges. This article must therefore be hereby marked "advertisement" in accordance with 18 U.S.C. Section 1734 solely to indicate this fact.

<sup>§</sup> The on-line version of this article (available at <http://www.jbc.org>) contains supplemental Figs. S1–S5.

<sup>†</sup> Recipient of a fellowship from the Universitat Autònoma de Barcelona.

<sup>‡</sup> Supported by a Ramón y Cajal project awarded by the MEC and co-financed by the Universitat Autònoma de Barcelona.

<sup>3</sup> To whom correspondence should be addressed: Institut de Biotecnologia i Biomedicina and Departament de Bioquímica i Biologia Molecular, Universitat Autònoma de Barcelona, 08193 Barcelona, Spain. Tel.: 34-93-581-1315; Fax: 34-93-581-2011; E-mail: FrancescXavier.Aviles@uab.es.

<sup>4</sup> The abbreviations used are: TCI, tick carboxypeptidase inhibitor; CP, carboxypeptidase; bCPA, bovine carboxypeptidase A; Ct, C-terminal domain; DTT, dithiothreitol; GdnHCl, guanidine hydrochloride; GdnSCN, guanidine thiocyanate; GSSG, oxidized glutathione; hCPB, human carboxypeptidase B; MALDI-TOF MS, matrix-assisted laser desorption/ionization-time of flight mass spectrometry; MCP, metalloproteinase; Nt, N-terminal domain; PDI, protein disulfide isomerase; RP-HPLC, reversed-phase high-performance liquid chromatography; TAFI, thrombin-activatable fibrinolysis inhibitor; MES, 4-morpholineethanesulfonic acid; GSH, reduced glutathione.

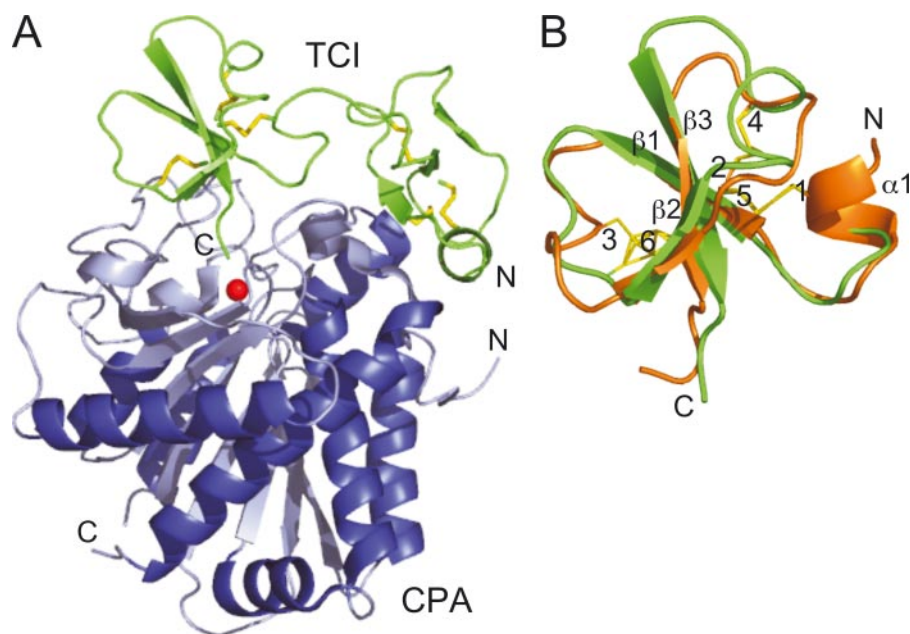


**FIGURE 1. Three-dimensional structure of TCI.** *A*, structure of the TCI-CPA complex shown in a ribbon representation. The helix and  $\beta$ -strands of TCI are shown in dark and light green, respectively, and the disulfide bonds are indicated in yellow. The helices and  $\beta$ -strands of bovine CPA are shown in dark and light blue, respectively, and the catalytic zinc atom is represented by a red sphere. The N and C termini of TCI and CPA are labeled. *B*, superposition of the N-terminal (orange) and C-terminal (light green) domains of TCI shown as ribbons. Cysteine residues, which are paired in a 1–5, 2–4, and 3–6 fashion in both molecules, are indicated in yellow. The secondary structure elements and the N-/C-terminal ends are labeled.

locarboxypeptidase inhibitor identified in the blood-sucking tick *Rhipicephalus bursa* (17). TCI strongly inhibits plasma CPB (known also as thrombin-activable fibrinolysis inhibitor, TAFI), a well known attenuator of fibrinolysis (18). It is therefore likely to be involved in the maintenance of the liquid state of blood during the feeding and digestion. Accordingly, we have recently shown that TCI stimulates fibrinolysis *in vitro* and thus may have potential for applications to prevent or treat thrombotic disorders (17). This 75-residue cysteine-rich protein constitutes a very interesting model of multidomain proteins, with two compact domains of similar size that display the same topology, but only share 27% of sequence identity (19). Each domain consists of a short  $\alpha$ -helix followed by a small twisted antiparallel  $\beta$ -sheet and is cross-linked by three disulfide bonds (Fig. 1). All six disulfide bonds seem to contribute to the high stability of the protein against temperature and denaturing agents. The crystal structures of TCI in complex with either bovine CPA or human CPB have revealed a double-headed binding mode not previously seen for the other CP inhibitors (20, 21): the C-terminal tail of TCI interacts with the active site of the enzyme in a way that mimics substrate binding, whereas the N-terminal domain binds to an exosite distinct from the active site groove.

Only the folding of single-domain disulfide-rich proteins has been characterized in depth to date. Therefore, TCI represents an attractive model system for understanding the folding and unfolding of both, multidomain and disulfide-rich proteins. The present work describes a detailed study of the oxidative folding and reductive unfolding of TCI. Kinetic, thermodynamic, structural, and functional analyses

of the two isolated domains, in comparison with the native protein, provide the biochemical basis for the two-domain nature of this inhibitor.

## EXPERIMENTAL PROCEDURES

**Protein Expression and Purification**—The synthetic gene cloned into the pBAT4-OmpA plasmid (17) was used as template to generate by PCR the constructs corresponding to the two protein domains of TCI. The N- (residues 1–36) and C-terminal (residues 37–75) domain constructs were verified by DNA sequencing. Complete TCI, and the two domains were obtained by heterologous expression in *Escherichia coli* strain BL21(DE3) using M9 minimal medium containing 0.5% glycerol and 0.2% casamino acids and inducing with 1 mM isopropyl 1-thio- $\beta$ -D-galactopyranoside (final concentration). The proteins were subsequently purified from the

extracellular medium by three chromatographic steps. Briefly, first the protein was applied into a Sep-Pak  $C_{18}$  cartridge (Waters) activated with 100% acetonitrile. The bound protein was washed with water followed by 10% acetonitrile, eluted with 30% 2-propanol, and then concentrated in a Rotavapor to remove the organic solvent. This initial step of purification was followed by a cation-exchange chromatography in a Sep-Pack CM cartridge (Waters), applying a gradient of 1 M NaCl in MES buffer (50 mM, pH 5.5). A final step of reversed-phase high performance liquid chromatography (RP-HPLC) in a 4.6-mm Protein C4 column (Vydac), using a linear gradient from 10–40% acetonitrile in 0.1% trifluoroacetic acid for 30 min, was performed to achieve maximal purity (>98%). Protein identity was confirmed by mass spectrometry (MS).

**Oxidative Folding**—Proteins (1 mg) were dissolved in Tris-HCl buffer (0.1 M, pH 8.4) containing 8 M guanidine hydrochloride (GdnHCl) and 100 mM dithiothreitol (DTT) and kept at 23 °C for 2 h. To initiate folding, the reduced and denatured sample was passed through a PD-10 column (Amersham Biosciences), previously equilibrated with Tris-HCl buffer (0.1 M, pH 7.4 or 8.4). The protein was then recovered in 1.2 ml and immediately diluted to a final protein concentration of 0.5 mg/ml in the same Tris-HCl buffer, both in the absence (*Control*–) and presence of redox agents: 0.25 mM 2-mercaptoethanol (*Control* +), 0.5 mM oxidized glutathione, or 0.5 mM/1 mM oxidized/reduced glutathione (GSSG/GSH). For some experiments, 4  $\mu$ M protein disulfide isomerase (PDI, Sigma) or selected concentrations of denaturants (0.5–5 M GdnHCl or 1–8 M urea) were added to the reaction. Folding intermediates were trapped in a time-course manner by mixing aliquots of the sample with 2% trifluoroacetic acid and analyzed

## Characterization of a Two-domain CP Inhibitor

by RP-HPLC as follows. A linear 10–40% gradient of acetonitrile containing 0.1% trifluoroacetic acid was applied during 50 min into a 4.6-mm Jupiter C4 column (Phenomenex) at a flow rate of 0.75 ml/min. Alternatively, folding intermediates were trapped by derivatization with vinylpyridine (0.2 M) in Tris-HCl buffer (0.1 M, pH 8.4) at 23 °C for 45 min, further diluted in 10 volumes of 0.1% trifluoroacetic acid, and analyzed by MS.

**Stop/Go Folding**—Acid-trapped intermediates were isolated by RP-HPLC as described under “Oxidative Folding,” freeze-dried, and allowed to continue the folding (at 23 °C) by dissolving the sample (0.5 mg/ml) in Tris-HCl buffer (0.1 M, pH 8.4), both in the absence (*Control*–) and presence (*Control*+) of 0.25 mM 2-mercaptoethanol. Folding intermediates were then similarly trapped by acidification and analyzed by RP-HPLC.

**Denaturation and Reductive Unfolding**—Native proteins were dissolved to a final concentration of 0.5 mg/ml in Tris-HCl buffer (0.1 M, pH 8.4) containing 0.25 mM 2-mercaptoethanol and selected concentrations of denaturants (0–8 M urea, 0–8 M GdnHCl, or 0–6 M guanidine thiocyanate (GdnSCN)). The reaction was allowed to reach equilibrium typically for 20 h at 23 °C. The samples were then quenched with 2% trifluoroacetic acid and analyzed by RP-HPLC using the conditions detailed under “Oxidative Folding.” For reductive unfolding experiments, native proteins (0.5 mg) were dissolved in 1 ml of Tris-HCl buffer (0.1 M, pH 8.4) with different concentrations of DTT (0.1–100 mM) at 23 °C. To monitor the kinetics of unfolding, time-course aliquots of the samples were likewise trapped with 2% trifluoroacetic acid and analyzed by RP-HPLC.

**Characterization of Peptide Ions Containing SH Groups and Disulfide Bonds**—The acid-trapped intermediates were purified by RP-HPLC and freeze-dried. Each sample (20 µg) was alkylated with 50 µl of vinylpyridine (0.2 M) in Tris-HCl buffer (0.1 M, pH 8.4) at room temperature (23 °C) for 45 min. The derivatized sample was then freed from reagents using a C<sub>18</sub> Zip-Tip pipette tip (Millipore) activated with 70% acetonitrile and equilibrated in 0.1% trifluoroacetic acid. Following protein adsorption and washing with 0.1% trifluoroacetic acid, the proteins were eluted with 3 µl of 70% acetonitrile containing 0.1% trifluoroacetic acid, dried, and treated with either trypsin or endoproteinase Lys-C (both sequencing grade, Roche Applied Science), at 1:20 (w/w) enzyme:substrate ratio, in Tris-HCl buffer (0.1 M, pH 8.4). Digestions were carried out at 37 °C for 15 h, and afterward the products were analyzed by matrix-assisted laser desorption/ionization-time of flight (MALDI-TOF) MS in a Voyager-DE Pro (Applied Biosystems). For disulfide bond assignments, digestion mixtures of non-reduced polypeptides were dissolved in 5 µl of HEPES buffer (10 mM, pH 9.0), reduced by addition of DTT (100 mM), and incubated at 65 °C for 15 min. For mass fingerprinting analysis, the reduced digestion mixtures were then freed from reagents using a C<sub>18</sub> Zip-Tip pipette tip as detailed above. 0.85 µl of the digests was spotted onto a MALDI-TOF sample holder, mixed with an equal volume of a saturated solution of  $\alpha$ -cyano-4-hydroxycinnamic acid (Sigma) in 50% acetonitrile containing 0.1% trifluoroacetic acid, dried, and analyzed with a MALDI-TOF MS operated in delayed extraction and reflector modes. The peptide mass fingerprint obtained was compared with the expected proteolytic digest of amino acids 23–97 (mature protein) of the

UniProtKB/TrEMBL entry Q5EPH2\_9ACAR (available at [ca.expasy.org/uniprot](http://ca.expasy.org/uniprot)) using the program PAWS (Proteometrics, available at [prowl.rockefeller.edu/](http://prowl.rockefeller.edu/)). All searches were constrained to a mass tolerance of 100 ppm. A tryptic peptide mixture of *Cratylia floribunda* seed lectin (SwissProt accession code P81517) prepared and previously characterized in our laboratory was used as mass calibration standard (mass range, 450–3300 Da) and used for mass fingerprinting. The sequence of selected peptides was determined by collision-induced dissociation by electrospray ionization tandem MS (MS/MS) using a QTrap instrument (Applied Biosystems) equipped with a nanoelectrospray source (Protana, Denmark). Double-charged ions selected after Enhanced Resolution MS analysis were fragmented using the Enhanced Product Ion with the Q<sub>0</sub> trapping option at 250 amu/s across the entire mass range. For MS/MS experiments, Q1 was operated at unit resolution, the Q1-to-Q2 collision energy was set to 35 eV, the Q3 entry barrier was 8 V, the linear ion trap Q3 fill time was 250 ms, and the scan rate in Q3 was 1000 amu/s. Product ion spectra were interpreted manually or using the on-line form of the MASCOT program at [www.matrixscience.com](http://www.matrixscience.com).

**Mass Spectrometry and NMR Spectroscopy**—The molecular masses of the recombinant proteins and the vinylpyridine-derivatized intermediates were determined by MALDI-TOF MS using a Bruker Ultraflex. Samples were prepared by mixing equal volumes of the protein solution and matrix solution: either  $\alpha$ -cyano-4-hydroxycinnamic acid (Sigma) or sinapic acid (Bruker) in 30% acetonitrile with 0.1% trifluoroacetic acid. For one-dimensional and two-dimensional NMR experiments, lyophilized proteins were dissolved to a final concentration of 3 mg/ml in H<sub>2</sub>O/D<sub>2</sub>O (9:1 ratio, v/v) containing 0.1% trifluoroacetic acid (pH 2.0). NMR spectra were acquired at different temperatures (25–90 °C) either on a Bruker ARX 400-MHz spectrometer or on a Bruker Avance 500-MHz spectrometer equipped with a CryoProbe. The collected spectra were processed and analyzed using the TopSpin v1.3 software packages from Bruker Biospin. one-dimensional and two-dimensional <sup>1</sup>H spectra were recorded using solvent-suppression WATERGATE techniques. The mixing times in TOCSY and NOESY experiments were set at 80 and 200 ms, respectively.

**CP Inhibitory Activity**—The inhibitory activity of folding intermediates and TCI domains was assayed by measuring the inhibition of the hydrolysis of the chromogenic substrate *N*-(4-methoxyphenylazoformyl)-Phe-OH by CPA and *N*-(4-methoxyphenylazoformyl)-Arg-OH by CPB at 350 nm. The assay was performed dissolving the substrates (both from Bachem) at a concentration of 0.1 mM in Tris-HCl buffer (50 mM, pH 7.5) containing 100 mM NaCl. The enzyme concentration was kept constant at ~2 nM, and increasing amounts of inhibitor were added. The equilibrium dissociation constants (*K<sub>i</sub>*) for the complexes were determined at the pre-steady state as described for tight binding inhibitors (22). Bovine CPA was purchased from Sigma, and human CPB was produced in the *Pichia pastoris* strain KM71 as published elsewhere in detail (23). The protein concentration of TCI and its two domains was determined based on the *A*<sub>280</sub> of the solution (calculated extinction coefficient of TCI: *E*<sub>0.1%</sub> = 0.97; C-terminal domain *E*<sub>0.1%</sub> = 1.45; and N-terminal domain *E*<sub>0.1%</sub> = 0.43).

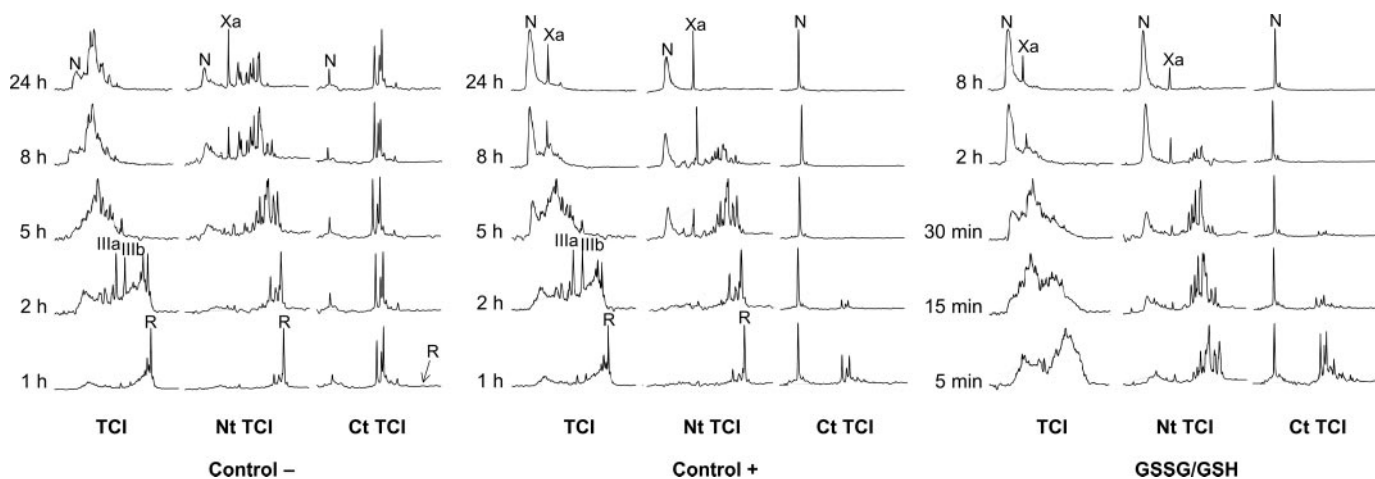


FIGURE 2. **Oxidative folding of TCI and TCI domains.** Folding was carried out in Tris-HCl buffer (pH 8.4) in the absence (*Control*−) and presence of either 2-mercaptoethanol (0.25 mM) (*Control* +) or GSSG/GSH (0.5 mM/1 mM). Acid-trapped intermediates were analyzed at the noted times by RP-HPLC as detailed under “Experimental Procedures.” *N* and *R* indicate the elution positions of the native and fully reduced forms, respectively. *IIIa* and *IIIb* are two major intermediates containing three native disulfide bonds. *Xa* is a scrambled isomer with six disulfide bonds.

## RESULTS

**Oxidative Folding of TCI**—Oxidative folding of reduced and denatured TCI was carried out in Tris-HCl buffer at pH 8.4 in the absence (*Control*−) or presence of different catalyst agents, namely, 2-mercaptoethanol (*Control* +), GSSG, or a mixture of GSSG and GSH. The intermediates that accumulate along the folding process were trapped by acidification in a time-course manner and subsequently analyzed by RP-HPLC. The chromatographic profiles of the refolding reactions are shown in Fig. 2. A high number of intermediates populate the early stages of TCI folding (up to 3 h), with similar RP-HPLC profiles regardless of the presence of 2-mercaptoethanol (see *Control*− and *Control* +). Importantly, two predominant fractions of intermediates, named *IIIa* and *IIIb*, accumulate significantly during these initial phases. The last stages of TCI folding are also characterized by a highly heterogeneous amount of intermediates; however, these intermediates accumulate to a lesser extent in the presence of a reducing agent (*Control* +). The addition of GSSG and GSSG/GSH strongly accelerates the formation of intermediates and the recovery of native protein. In contrast, and unlike in other model proteins like leech carboxypeptidase inhibitor (24), the addition of selected concentrations of denaturant (0–2 M urea, 0–1 M GdnHCl) does not significantly affect the folding reaction through the destabilization of intermediates (data not shown).

To evaluate the disulfide bond content of the folding intermediates, the reactions were trapped by alkylation with vinylpyridine at selected time points and further analyzed by MS. The results show a sequential formation of 1-, 2-, 3-, 4-, 5-, and 6-disulfide intermediates that lead to the native structure (Fig. 3). The folding of TCI cannot reach completion in the absence of catalysts, indicated by the fact that only ~15% of the protein is recovered as native form after 48 h of reaction (Fig. 2, *Control*−). The rest of the protein remains trapped as a mixture of non-native 6-disulfide (scrambled) isomers that need the presence of redox agents to reshuffle their disulfide bonds and reach the native state. Thus, the conversion of these isomers to the native protein constitutes the major rate-limiting step of the

folding process. The presence of catalysts not only promotes the recovery of native TCI (~85% in *Control* + and GSH/GSSG) but also the accumulation of another species at the end of the folding reaction. This species, named *Xa*, is a 6-disulfide scrambled isomer, based on vinylpyridine derivatization coupled to MS analysis, and represents ~10% of the total protein. *IIIa* and *IIIb* intermediates were separated from other species by treatment with vinylpyridine and RP-HPLC, which allowed us to determine that they contain three disulfide bonds. Their disulfide pairings were determined by digestion with trypsin and Lys-C, followed by mass fingerprint analysis and peptide sequencing (for details, see “Experimental Procedures”). These studies revealed that both species comprise three native disulfide bonds in one domain and no disulfide bonds in the other domain. *IIIa*: Cys<sup>3</sup>–Cys<sup>31</sup>, Cys<sup>10</sup>–Cys<sup>27</sup>, and Cys<sup>16</sup>–Cys<sup>32</sup>; *IIIb*: Cys<sup>40</sup>–Cys<sup>70</sup>, Cys<sup>47</sup>–Cys<sup>64</sup>, and Cys<sup>54</sup>–Cys<sup>71</sup>. The list of peptides used for disulfide assignments is given in Table 1 and the MS spectra in the supplemental materials.

Because it was unlikely that the pathway of TCI to its functional conformation within the cell was as inefficient as reported above, the influence of the protein folding catalyst PDI was also investigated at pH 7.4 to mimic physiological conditions. As shown in Fig. 4, the addition of PDI has a dramatic effect on the final recovery of native TCI: 70% versus 6% in the presence and absence of PDI, respectively (*Control*−). Remarkably, the presence of PDI combined with GSH/GSSG strongly prevents the accumulation of the *Xa* scrambled isomer.

**Oxidative Folding of TCI Domains**—To dissect the contribution of each individual domain in the folding of TCI, the oxidative folding of both isolated domains (N- and C-terminal domains, abbreviated here as Nt and Ct, respectively) was performed in Tris-HCl buffer (pH 8.4) in the absence (*Control*−) or presence of catalyst agents. For the two domains, the RP-HPLC analysis of the acid-trapped intermediates showed a lower accumulation of intermediates along the folding reaction, as compared with that of the complete TCI (Fig. 2). The folding of Nt and Ct TCI undergoes a sequential conversion of 1-, 2-,

## Characterization of a Two-domain CP Inhibitor

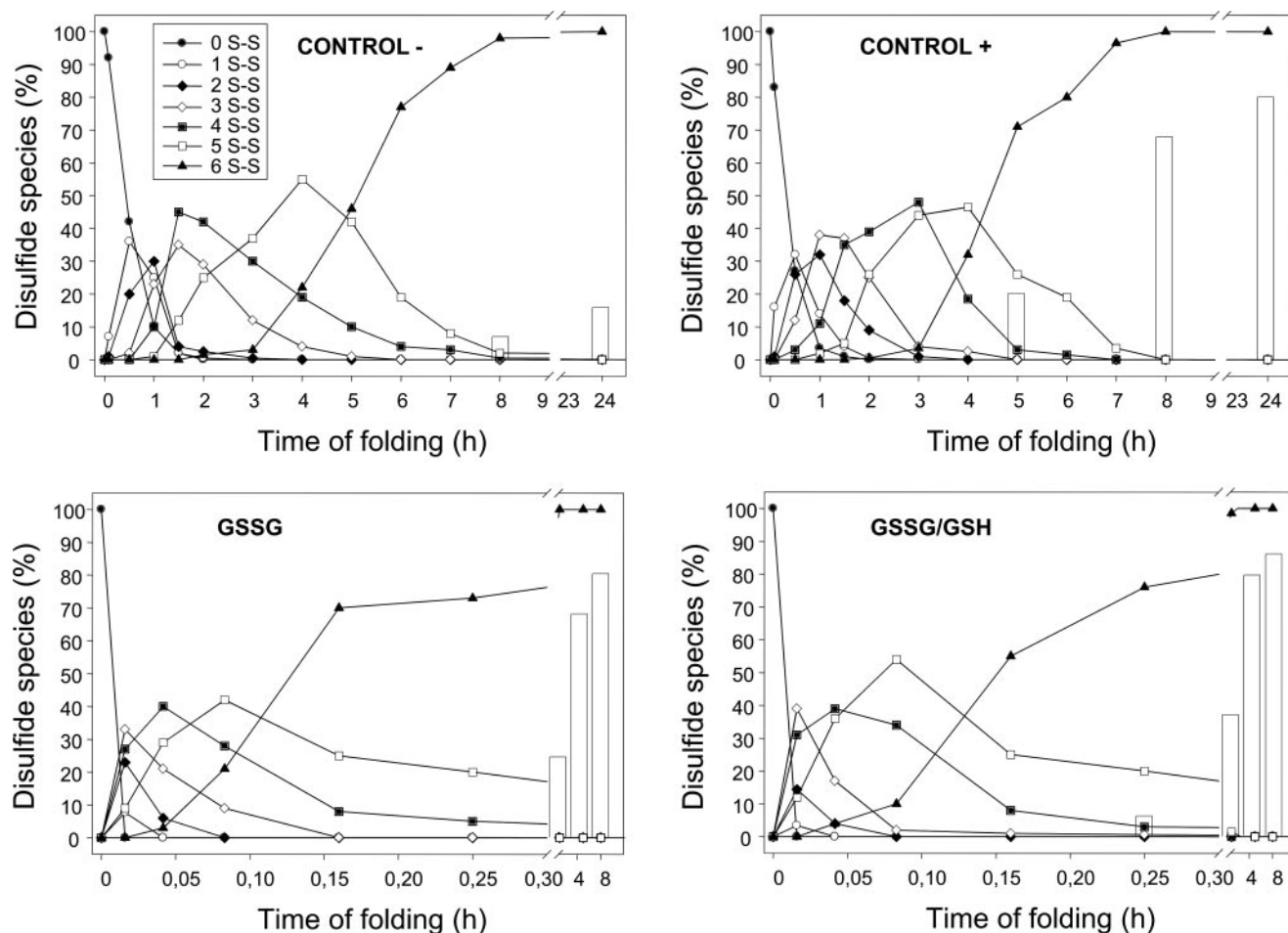


FIGURE 3. **Disulfide species along the oxidative folding of TCI.** Folding was performed in Tris-HCl buffer (pH 8.4) in the absence (*Control* -) and presence of redox agents: 2-mercaptoethanol (0.25 mM) (*Control* +), GSSG (0.5 mM), or GSSG/GSH (0.5 mM/1 mM). *X S-S* represents an ensemble of species with *X* disulfide bonds. The 6-disulfide species includes the native form and all scrambled isomers. Quantitative analysis of disulfide species was based on the peak response of MALDI-TOF spectra (data not shown). The recovery of native form is represented by bars and was calculated from the peak areas in the corresponding RP-HPLC chromatograms.

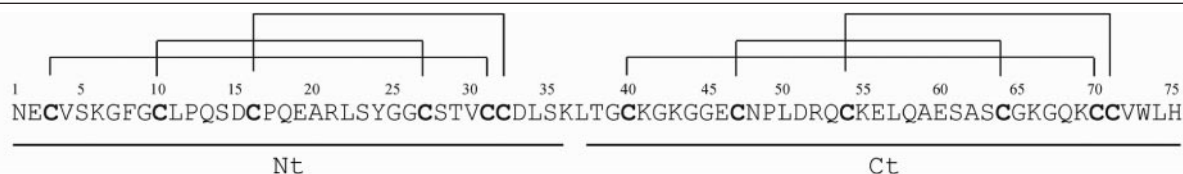
and 3-disulfide intermediates to reach the native form, based on vinylpyridine alkylation and MS analysis (data not shown). In the case of Nt TCI, at the beginning of the folding process (up to 3 h) the RP-HPLC profiles were similar both in *Control* - and *Control* + experiments. It is at the last stages of folding when 3-disulfide (scrambled) isomers accumulate strongly hindering the recovery of native protein (~20% at 48 h in *Control* -). Similar to TCI, the addition of redox agents greatly facilitated the conversion to the native structure, allowing a recovery of >80% in the presence of GSSG/GSH. It is worth mentioning that another species (a scrambled isomer) significantly accumulated at the end of the folding reaction together with the native form of Nt TCI (Fig. 2). Ct TCI refolds rapidly through a limited number of disulfide intermediates. Nevertheless, the folding reaction cannot reach completion and only ~10% of the protein attains the native conformation in the absence of redox agents (*Control* -). Like in the cases of TCI and Nt TCI, most of the protein remained trapped as scrambled isomers; therefore the addition of a reducing agent strongly favors the recovery of the native protein. Remarkably, under these redox conditions all Ct TCI reached the native state (Fig. 2, *Control* + and GSSG/GSH).

The oxidative folding of Nt and Ct TCI correlates with the results obtained from the stop/go experiments of IIIa and IIIb intermediates. These two species were isolated and allowed to resume their folding in the absence (*Control* -) and presence (*Control* +) of 2-mercaptoethanol (Fig. 5). In both conditions, IIIa, containing the same disulfide bonds as Nt TCI, folds through a few intermediates that lead to the formation of the other domain. The presence of reducing agent accounts for an almost complete recovery of native protein by promoting reshuffling of scrambled isomers. IIIb, containing the same disulfide bonds as Ct TCI, displays a more heterogeneous population of intermediates along its folding reaction. A final accumulation of scrambled isomers, strongly prevented by the addition of 2-mercaptoethanol, was observed as in the case of IIIa. However, the recovery of native protein was limited by the formation of a stable scrambled intermediate, which is analog to that found in the oxidative folding of TCI and Nt TCI.

**Reductive Unfolding of TCI and TCI Domains**—Reductive unfolding of native TCI was carried out in Tris-HCl buffer at pH 8.4 using increasing concentrations of DTT as reducing agent. The unfolding intermediates were quenched by acidification in a time-

**TABLE 1**
**Assignment of peptide fragments from IIIa and IIIb intermediates**

Peptides were generated by incubation with vinylpyridine in non-reducing (A) and reducing (B) conditions and subsequent digestion with sequencing grade bovine trypsin and endoprotease Lys-C. Fragments containing pyridylethyl (PE-) cysteines, sulfhydryl groups (SH), and disulfide bonds (S-S) were analyzed by MALDI-TOF MS. Fragment limits refer to the amino acid sequence numbering of the mature protein (UniProtKB/TrEMBL entry Q5EPH2\_9ACAR).



M+H <sup>+</sup>	Trypsin		Endo Lys-C	
	PE-IIIa	PE-IIIb	PE-IIIa	PE-IIIb
A				
784.4		1-6 (C <sup>3</sup> -PE)		
970.5	70-75 (C <sup>70,71</sup> )-PE		70-75 (C <sup>70,71</sup> )-PE	
1065.5	44-52 (C <sup>47</sup> -PE)			
1227.6	56-66 (C <sup>64</sup> -PE)		56-66 (C <sup>64</sup> -PE)	
1605.7*	7-21 (C <sup>10</sup> -C <sup>16</sup> )			
1529.8			44-55 (C <sup>47,54</sup> )-PE	
1817.9		7-21 (C <sup>10,16</sup> )-PE		
1850.9		22-36 (C <sup>27,31,32</sup> )-PE		
3648.8		7-36 (C <sup>10,16,27,31,32</sup> )-PE		7-36 (C <sup>10,16,27,31,32</sup> )-PE
3778.7			1-36 (C <sup>3,10,16,27,31,32</sup> ) (3 S-S)	
3796.6	1-21+22-36 (3 S-S)		1-21+22-36 (3 S-S)	
3814.6	1-7+8-21+22-36 (3 S-S)			
3908.7		37-73 (3 S-S)		
4158.8		37-75 (3 S-S)		
4385.9	1-41 (3 S-S, C <sup>40</sup> -PE)			
B				
970.5	70-75 (C <sup>70,71</sup> )-PE		70-75 (C <sup>70,71</sup> )-PE	
1065.5	44-52 (C <sup>47</sup> -PE)			
1227.6			56-66 (C <sup>64</sup> -PE)	
1319.6				44-55 (C <sup>47,54</sup> )-SH
1529.8			44-55 (C <sup>47,54</sup> )-PE	
1535.1	22-36 (3 SH)			
1607.7	7-21 (C <sup>10,16</sup> )-SH			
1817.9		7-21 (C <sup>10,16</sup> )-PE		
2267.9	1-21 (3 SH)			
2322.3			37-55 (C <sup>40,47,54</sup> )-PE	
2736.3		44-69 (3 SH)		
2921.3		42-69 (3 SH)		42-69 (3 SH)
3123.1	7-36 (5 SH)		7-36 (5 SH)	
3423.6		37-69 (4 SH)		
3648.8				7-36 (C <sup>10,16,27,31,32</sup> )-PE
3731.1	7-41 (5 SH, C <sup>40</sup> -PE)			
3783.9	1-36 (6 SH)		1-36 (6 SH)	
4164.9		37-73 (6 SH)		
4391.9	1-41 (6 SH, C <sup>40</sup> -PE)			

\* , minor species

course manner and analyzed by RP-HPLC. Different fractions of intermediates were detected along the process (Fig. 6); among them, two fractions with an HPLC elution time equivalent to that of the IIIa and IIIb intermediates were found to accumulate strongly. Subsequent disulfide assignment of these two species

confirmed that they are indeed identical to the predominant 3-disulfide intermediates of TCI oxidative folding (data not shown). Similar RP-HPLC profiles were observed when the unfolding reaction was performed in the presence of different concentrations of DTT (from 0.5 to 100 mM).

## Characterization of a Two-domain CP Inhibitor

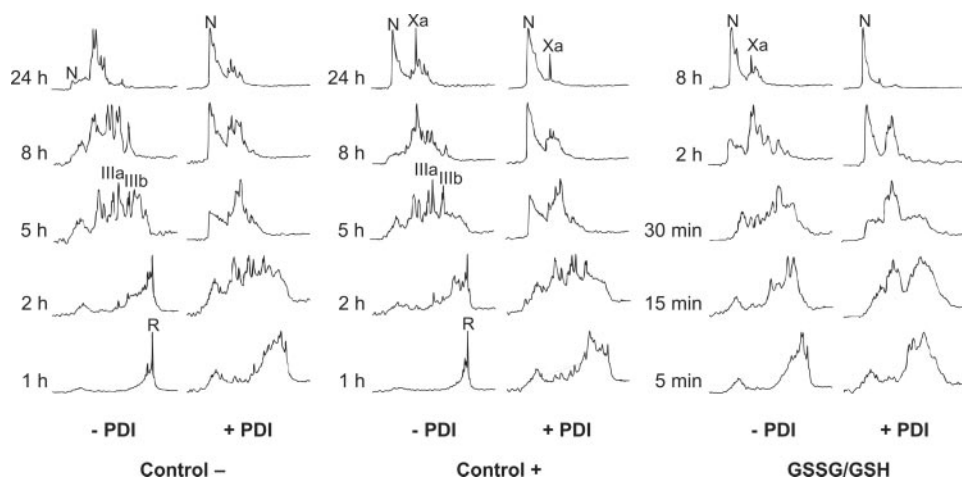


**FIGURE 4. Oxidative folding of TCI in the presence of PDI.** Folding was carried out in Tris-HCl buffer (pH 7.4) in the absence (*Control*−) and presence of either 2-mercaptoethanol (0.25 mM) (*Control*+) or GSSG/GSH (0.5 mM/1 mM). The effect of the folding catalyst PDI (4  $\mu$ M) was tested. Acid-trapped intermediates were analyzed in a time-course manner by RP-HPLC. *N* and *R* indicate the elution positions of the native and fully reduced forms of TCI, respectively. *IIIa* and *IIIb* are two intermediates with three native disulfide bonds, while *Xa* is a scrambled isomer.

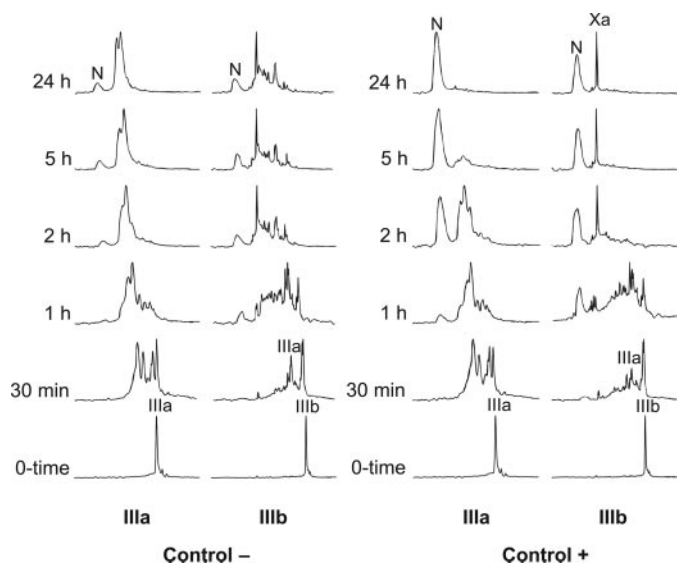


**FIGURE 5. Stop/go folding of *IIIa* and *IIIb* intermediates of TCI.** Both intermediates were trapped by acidification, purified by RP-HPLC, freeze-dried, and dissolved in Tris-HCl buffer (pH 8.4) to allow folding either in the absence (*Control*−) or presence (*Control*+) of 2-mercaptoethanol (0.25 mM). Folding intermediates were then similarly trapped with acid and analyzed by RP-HPLC. *N*, *IIIa*, *IIIb*, and *Xa* stand for the native form, two 3-disulfide intermediates, and a scrambled isomer of TCI, respectively.

Reductive unfolding of purified *IIIa* and *IIIb* intermediates was also carried out at pH 8.4 using various concentrations of DTT (in supplemental materials). In all conditions, the reduction of their three native disulfide bonds undergoes an apparent “all-or-none” mechanism in which only low amounts of partially reduced intermediates accumulate (25). Interestingly, a minor interconversion from *IIIb* to *IIIa* can be observed before the concerted reduction of its disulfide bonds.

Reductive unfolding of Nt and Ct TCI, corresponding to the folded domains in *IIIa* and *IIIb*, respectively, in terms of disulfide bond content, also occurred in a cooperative manner without significant accumulation of 1- or 2-disulfide intermediates

(Fig. 6). Comparison of the analyses conducted on the different proteins revealed that native TCI resists slightly higher concentrations of DTT than the intermediates and the Nt domain, which present a very similar stability. Surprisingly, native Ct TCI resists higher concentrations of DTT than the complete TCI: similar percentages of unfolded protein were obtained using 10 mM and 2 mM DTT for Ct and TCI, respectively.

**Conformational Stability of TCI and TCI Domains**—In the presence of denaturant and thiol initiator, unfolding of a native disulfide-containing protein is accompanied by reshuffling of its native disulfide bonds (process called “disulfide scrambling”) (26, 27). On this basis,

denaturation of native TCI was performed in the presence of increasing concentrations of denaturant and 0.25 mM 2-mercaptoethanol at pH 8.4. After reaching equilibrium, the reactions were analyzed by RP-HPLC (see the profiles in the supplemental materials). The extent of unfolding, and hence the equilibrium constant between native TCI and scrambled isomers, was clearly dependent upon the strength of the denaturant (Fig. 7). The concentrations of GdnSCN and GdnHCl required to achieve 50% denaturation were 2.5 and 5.4 M, respectively. Urea was unable to denature significantly the native TCI. The denaturation curves for Nt and Ct TCI were similarly determined (Fig. 7). The former domain exhibited a much lower stability compared with native TCI against the same denaturing agents, with the following midpoint denaturant concentrations: 1.6, 3.5, and 6.5 M for GdnSCN, GdnHCl, and urea, respectively. The other TCI domain, Ct, resists very high concentrations of denaturant, and only the presence of 5.3 M GdnSCN could render 50% denaturation.

In addition to the disulfide scrambling experiments, the conformational stability of both TCI domains was also investigated by NMR spectroscopy. Native TCI shows an extreme resistance to temperature, as demonstrated by a similar shape/dispersion of the one-dimensional spectrum at 25 and 90 °C (17). Nt and Ct TCI spectra were dramatically affected after raising the temperature from 25 to 90 °C (see supplemental materials). Although both domains were denatured, Ct TCI resisted higher temperatures in comparison with Nt TCI.

**Conformational Properties of TCI Domains**—The  $^1\text{H}$  NMR spectrum of TCI showed a wide signal dispersion of resonances at both the low and high fields, with a significant number of potential methyl protons in the 0- to 1-ppm region and rich in exchangeable resonances in the NH region (Fig. 8). The spectra of *IIIa* and *IIIb* intermediates, as well as of Nt and Ct TCI, display a wide upfield/downfield signal dispersion, although it is appreciably smaller than that of the native protein. They also show excellent peak sharpness, which is a clear indication that these species are properly folded or very close to that. In con-

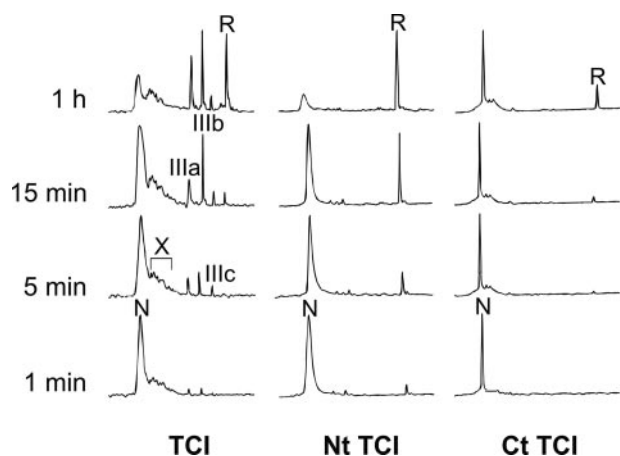


FIGURE 6. **Reductive unfolding of TCI and TCI domains.** The native form of TCI and TCI domains was treated with 10 mM DTT in Tris-HCl buffer (pH 8.4). Time-course intermediates were trapped by acidification and analyzed by RP-HPLC. *N* and *R* stand for the native and reduced forms. *X* stands for an ensemble of 6-disulfide (scrambled) isomers. *IIIa*, *IIIb*, and *IIIc* are 3-disulfide intermediates.

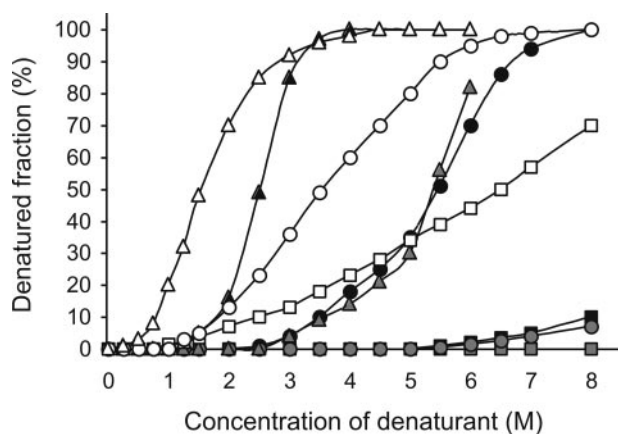


FIGURE 7. **Denaturation curves of TCI and TCI domains.** Denatured fraction is the percentage of native protein that is converted to scrambled isomers. Curves for TCI, Nt, and Ct domains are depicted with black, white, and gray symbols, respectively. The denaturants used are GdnSCN ( $\blacktriangle$ ), GdnHCl ( $\bullet$ ), and urea ( $\blacksquare$ ). Denaturation was carried out at 23 °C, for 20 h, in Tris-HCl buffer (0.1 M, pH 8.4) containing 2-mercaptoethanol (0.25 mM) and the indicated concentration of denaturant.

trast, the Xa scrambled isomer spectrum exhibits a partial band broadening and peak collapse, together with a low chemical shift dispersion (Fig. 8), indicating that this intermediate is partially folded.

The comparison of the two-dimensional NMR spectra of IIIa and IIIb with those of Nt and Ct TCI support the idea that both intermediates comprise a native-like structure of one of the two TCI domains (spectra included in supplemental materials). Most of the NOE contacts observed in the fingerprint region of the IIIa two-dimensional spectrum are also found in similar positions of the Nt two-dimensional spectrum. The same observation can be applied to IIIb and Ct TCI. Although there are no significant chemical shifts of the common  $C\alpha$  and NH cross-peaks in the intermediates and isolated domains, numerous contacts can be observed in the central region of the IIIa and IIIb fingerprint spectra. This is probably related to the misfolded Nt and Ct domains present in IIIb and IIIa intermediates, respectively. Also, the higher degree of dispersion and number

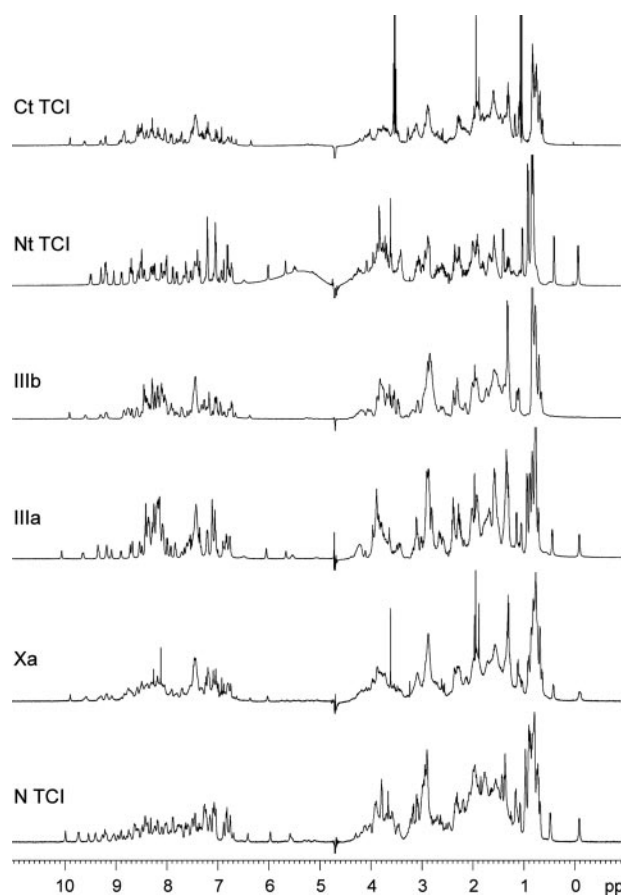


FIGURE 8.  **$^1\text{H}$  NMR analysis of the different TCI forms.** One-dimensional spectra of native TCI, Xa, IIIa, IIIb, Nt, and Ct TCI (3 mg/ml) were recorded in a 500-MHz Bruker NMR spectrometer. Spectra were obtained at 25 °C in  $\text{H}_2\text{O}/\text{D}_2\text{O}$  (9:1 ratio, v/v) containing 0.1% trifluoroacetic acid (pH 2.0).

of NOE contacts displayed by IIIb and Ct TCI, together with stronger cross-peaks corresponding to aliphatic side chains, clearly indicate that this domain is more compact than the Nt one.

On the other hand, the two-dimensional spectrum of the Xa scrambled isomer displays many similarities with that of IIIb and Ct TCI. Most of the cross-peaks found in the 6.0- to 7.5- and 9.0- to 10.0-ppm regions are common among these three TCI forms. This is in accordance with the folding results that point out the Nt domain as the last one to be formed. Thus, it seems that Xa contains a native-like Ct domain and mispaired disulfide bonds in the other domain. Because previous circular dichroism measurements had indicated that TCI essentially has the same conformation in a wide pH range (2.0–8.0) (17), all TCI species were analyzed in acidic solution to avoid the conversion of intermediates into native protein.

**CP Inhibition by TCI Domains**—TCI is a tight binding, competitive inhibitor of metalloproteases of the A/B subfamily with  $K_i$  values in the nanomolar range. Here, we demonstrate that the N peak is indeed the naturally occurring inhibitor, because it has the same activity, disulfide pairing, and elution position in HPLC than the protein isolated from tick extracts (data not shown). In addition, the peak that elutes together with N (e.g. in Fig. 4) corresponds to the native protein lacking the last residue (His<sup>75</sup>), based on MS analysis. Similar to

## Characterization of a Two-domain CP Inhibitor

potato carboxypeptidase inhibitor and leech carboxypeptidase inhibitor, the removal of the C-terminal residue does not significantly affect its affinity toward carboxypeptidases (17).

Equilibrium dissociation constants for the complexes of the major folding intermediates and domains of TCI with bovine carboxypeptidase A (bCPA) and human carboxypeptidase B (hCPB) were measured using a pre-steady-state approach. As shown in Table 2, the inhibitory potential of the Xa scrambled isomer was very similar to that of native TCI. Likewise, IIIb, comprising native disulfide bonds in the C-terminal domain, inhibited carboxypeptidases A and B with a nanomolar  $K_i$ . In contrast, in Ct TCI the absence of the N-terminal domain is accompanied by a significant loss of inhibitory activity, with a ~13-fold higher  $K_i$  compared with that of native TCI. An even worse inhibition was observed for IIIa, which lacked the disulfide bonds in the C-terminal domain. Finally, as it was expected, the N-terminal domain of TCI and its major scrambled isomer (Xa Nt) did not inhibit at all any of the assayed carboxypeptidases. These results correlate well with the binding mode and inhibition of TCI toward metallo-carboxypeptidases (Fig. 1A).

### DISCUSSION

TCI provides an interesting system to characterize the folding of two-domain disulfide-rich proteins, much less studied than the single-domain ones. The folding of TCI proceeds from the reduced protein to the native state through a sequential oxidation of cysteine residues, with the presence of intermediates comprising one to six disulfide bonds (summarized in Fig. 9). The most important intermediates that accumulate along its folding (IIIa and IIIb) are 3-disulfide species containing the native disulfide bonds of the Nt and Ct domains of TCI, respec-

**TABLE 2**  
Inhibition constants ( $K_i$ ) of TCI forms against bovine CPA and human CPB

	$K_i$						
	Native TCI	Xa	IIIa	IIIb	Ct TCI	Nt TCI	Xa Nt
			NM				
bCPA	1.1 ± 0.3	1.6 ± 0.4	19.8 ± 1.2	3.3 ± 0.5	13.8 ± 1.3	NI <sup>a</sup>	NI
hCPB	1.3 ± 0.2	3.5 ± 0.5	38.5 ± 1.8	8.8 ± 0.7	36.5 ± 1.9	NI	NI

<sup>a</sup> NI, no inhibition at 100  $\mu$ M concentration of inhibitor.

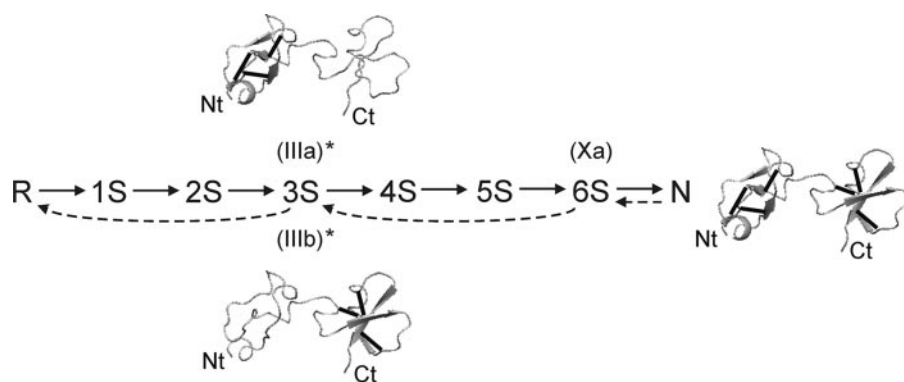


**FIGURE 9. Scheme of TCI folding.** The oxidative folding and reductive unfolding pathways of TCI are shown as solid and dashed arrows, respectively. R and N indicate the reduced and native forms of this protein. XS are ensembles of molecules with X number of disulfide bonds. The asterisks refer to intermediates containing exclusively native disulfide bonds. The localization of disulfides for IIIa, IIIb, and N is indicated in the native structure of TCI.

tively. The lack of well populated intermediates with crossed disulfide bonds between both domains indicates that the folding of TCI domains takes place independently, without an extensive interaction between both moieties. This is further confirmed by the fact that both isolated domains of TCI can reach their respective native state individually, in the absence of the other domain. Taken together, the folding of TCI can be seen as the sum of the folding pathways of its two domains, without any need of cooperativity among them and without any fundamental role of the connecting loop in the overall folding process.

The most predominant scrambled isomer observed in TCI folding (Xa) corresponds to a species with a properly paired Ct domain and a "scrambled" Nt domain, based on both stop/go and two-dimensional NMR experiments. This fact, together with the observation that Xa is also detected in the folding of Nt TCI but not in that of the Ct domain, confirms that TCI folding involves two independent folding events. The Ct domain folds 15 times faster than the Nt one, which indicates that the acquisition of the proper disulfide pairing in the latter constitutes the rate-limiting step of the process. The folding rate of a two-domain protein whose domains fold independently is expected to be the one corresponding to its slower folding domain. Accordingly, the folding rates of TCI and Nt TCI are nearly the same. The slow *in vitro* folding kinetics of TCI is strongly accelerated by the presence of PDI, which catalyzes the formation and isomerization of disulfide bonds in the eukaryotic endoplasmic reticulum (28, 29). In the presence of redox agents and PDI, even the most stable scrambled isomer (Xa) is reshuffled to native TCI. Due to the high content of disulfide bonds and the metastability of its folding intermediates, PDI probably assists the *in vivo* folding of TCI, thus avoiding the accumulation of misfolded protein and its subsequent aggregation, as similarly observed for lysozyme and ribonuclease A (30, 31).

TCI disulfide bonds are buried in the native protein, therefore their partial reduction must be accompanied by a global unfolding process. The major intermediates observed in the reductive unfolding of TCI are IIIa and IIIb, the same intermediates that populate TCI folding, indicating that TCI unfolding proceeds through two main local unfolding events. The lack of detectable intermediates with 1-, 2-, 4-, or 5-disulfide bonds

implies that each local unfolding event corresponds mainly to the global unfolding of one TCI domain, which would be in accordance with its oxidative folding that also proceeds through two independent folding events. According to this assumption, TCI should be expected to resist as much DTT as its more stable domain. Nevertheless, Ct TCI resists higher concentrations of DTT that both TCI and IIIb in which the Ct domain is properly folded. This indicates that in IIIb, the unfolded Nt domain has a destabilizing effect on the properly folded Ct domain. This effect would

also be present during TCI unfolding, thus explaining why its stability is lower than that of Ct TCI. Whether this effect results from a local increase of free thiol concentration upon reduction of disulfide bonds in Nt, suggesting transient contacts between the flexible unfolded Nt sequence and the properly folded Ct domain during TCI reductive unfolding, or it just corresponds to an entropic effect, still remains to be clarified.

TCI and its domains display a high stability against denaturation by different chaotropic agents, based on the disulfide scrambling data and the NMR analysis. The one-dimensional NMR spectra at raising temperatures show that the NH protons display a high resistance to exchange with the solvent, with a significant number of resonances at both the low and high fields at 70 °C and in the case of native TCI even at 90 °C (17). All proteins recuperate most of their signal dispersion of resonances after decreasing the temperature at 25 °C, indicating that their thermal unfolding is reversible. The disulfide scrambling data also confirm their high stability in the presence of different denaturants. This high stability is probably related to the presence of a high density of disulfide bonds, which stabilize proteins in two ways: reducing the entropy of the unfolded state, thus destabilizing it and also stabilizing the folded state favoring local interactions (32, 33). Surprisingly, the stability of the Nt and Ct domains exhibit dramatic differences compared with each other, with the Ct domain resisting much higher concentrations of denaturant than the Nt one. Both domains display a similar structure (root mean square deviation of 1.26 Å for backbone atoms; Fig. 1B) and an analogous architecture of disulfide bonds. Thus, their amino acid composition and/or some particular local conformational features are likely to affect their stability. To provide insights into the reasons underlying this difference, we analyzed both domains using FoldX, an empirical force field used for energy calculations in proteins (<http://foldx.embl.de/>; (34)). In good agreement with the experimental data, the computational algorithm predicts the Ct domain of TCI to be 5 times more stable than the Nt one. Actually, the Ct domain of TCI, with a midpoint denaturant concentration of 5.3 M for GdnSCN, is one of the most stable protein ever described (35). A detailed analysis of the energy terms predicted by FoldX points at differences in the main chain entropy and desolvation of the backbone polar groups as the main factors accounting for the observed divergent stabilities. In this regard, the loops closed by the first and the last disulfide bonds in the Ct domain (Cys<sup>40</sup>–Cys<sup>70</sup> and Cys<sup>54</sup>–Cys<sup>71</sup>) are longer than those in the Nt domain (Cys<sup>3</sup>–Cys<sup>31</sup> and Cys<sup>16</sup>–Cys<sup>32</sup>). This is likely to result in a more compact conformation derived from a stronger entropy reduction of its unfolded state, which is herein supported by the two-dimensional NMR data.

For a given fold, a higher stability usually correlates with faster folding rates and slower unfolding speed (36). This is the case of TCI domains, because the folding of Ct TCI is faster and more efficient than that of the Nt domain, especially in the presence of redox agents, and also the reductive unfolding of Ct TCI is much slower than the one of its Nt counterpart. The disparity in the folding kinetics of both domains could be one of the most important factors accounting for the particular folding pathway of TCI. As previously discussed, one of the most striking features of TCI folding is the lack of stable intermedi-

ates with disulfide bonds connecting the two domains. If we take into account that in the reduced and unfolded protein Cys<sup>31</sup> and Cys<sup>32</sup> (Nt domain) are sequentially closer to Cys<sup>40</sup> (Ct domain) than to their respective partners, the lack of intermediates with crossed disulfide bonds would be hardly explainable in entropic terms if TCI folded at once. However, a strong bias of the unfolded Ct domain toward the native conformation, together with a fast folding rate would result in properly connected and highly buried cysteines in the Ct part, precluding the formation of inter-domain disulfides during the subsequent steps of folding. This fast “locking in” of the Ct disulfides, combined with a probably less native biased folding of the Nt domain, would explain the accumulation of a stable scrambled isomer (Xa) and also the acquisition of native protein from Nt without altering the already formed Ct domain. Thus, it is likely that the observed independent folding of both TCI domains is mainly determined by their very different folding kinetics. This strategy would avoid the accumulation of misfolded forms comprising inter-domain disulfides, which could complicate enormously and unnecessarily the TCI folding reaction.

The <sup>1</sup>H NMR and inhibitory activity data of IIIa and IIIb intermediates indicate that they are active forms with native disulfide pairings at the Nt and Ct folded TCI domains, respectively. The observation that the *K<sub>i</sub>* of the IIIb intermediate is 5-fold lower than that of IIIa, together with the lack of inhibition exhibited by the Nt domain, are in agreement with the primary interaction of the Ct tail of TCI with the active site groove of the CP (37). Also, both TCI intermediates show a better *K<sub>i</sub>* than their respective Nt and Ct domains, indicating that the improperly folded domains in the intermediates also contribute to CP inhibition. Finally, the 13-fold higher *K<sub>i</sub>* of Ct TCI in comparison to native TCI reflects the importance of the secondary contacts established between the Nt domain and the enzyme surface. Taken together, these observations conclude that TCI inhibits CPs in a double-headed fashion, with strong contributions coming from both domains, as recently described from the x-ray structure of its complex with hCPB and bCPA (19). On the other hand, Ct TCI inhibits bCPA with a 3-fold lower *K<sub>i</sub>* than hCPB, a difference not previously observed in the case of native TCI, which indicates that the two-domain architecture of TCI not only affects its binding affinity but also its specificity toward CPs.

TCI domains are extremely stable molecules structurally related to the β-defensin-fold family, which includes many proteins that act in harsh environments (38). Ct TCI shows a higher stability, a faster folding kinetics, and the same folding efficiency as native TCI, thereby the two-domain nature of TCI cannot be related to an optimization of either conformational or folding properties. Its two-domain nature probably answers the need to improve its inhibitory capability. Thus, the independent folding of the two domains renders a native TCI with a better inhibitory potential without dramatically affecting its folding rate, as it would be expected from the 2-fold increase in the number of disulfide bonds. The faster Ct folding rate prevents inter-domain disulfide formation, diminishing the number of possible folding intermediates and lowering the complexity of TCI folding landscape. As a result, TCI is a quite efficient folding molecule compared with Ct TCI, with a signif-

## Characterization of a Two-domain CP Inhibitor

icantly lower  $K_i$  against CPs owing to the numerous interactions established between the Nt domain and the enzyme surface, which lead to a highly efficient double-headed binding.

As mentioned above, the  $K_i$  improvement is stronger in the case of hCPB, the carboxypeptidase most closely related to TAFI (48% sequence identity) (39). TAFI constitutes a risk factor for thrombosis and coronary artery disease, and its inhibition leads to an enhancement of clot lysis (40, 41). The double-headed architecture provides TCI with a 5-fold lower  $K_i$  toward TAFI compared with potato carboxypeptidase inhibitor and a 10-fold acceleration of fibrinolysis with respect to this single-headed inhibitor used as a model in thrombolytic assays (42, 43). In this way, and as previously discussed, the Nt domain could also contribute to improve the affinity/modulate the specificity of TCI toward CPBs, constituting a good target for the design of new TCI molecules to be used as thrombolytic drugs.

*Acknowledgments*—We thank Dr. T. Parella for his help with the NMR experiments and Dr. J. Vendrell for many helpful discussions and insights.

### REFERENCES

1. Onuchic, J. N., and Wolynes, P. G. (2004) *Curr. Opin. Struct. Biol.* **14**, 70–75
2. Ross, C. A., and Poirier, M. A. (2004) *Nat. Med.* **10**, (suppl.) S10–S17
3. Arolas, J. L., Aviles, F. X., Chang, J. Y., and Ventura, S. (2006) *Trends Biochem. Sci.* **31**, 292–301
4. Creighton, T. E. (1997) *Biol. Chem.* **378**, 731–744
5. Chang, J. Y. (2002) *J. Biol. Chem.* **277**, 120–126
6. Chatrenet, B., and Chang, J. Y. (1993) *J. Biol. Chem.* **268**, 20988–20996
7. Creighton, T. E. (1992) *Science* **256**, 111–114
8. van den Berg, B., Chung, E. W., Robinson, C. V., and Dobson, C. M. (1999) *J. Mol. Biol.* **290**, 781–796
9. Welker, E., Narayan, M., Wedemeyer, W. J., and Scheraga, H. A. (2001) *Proc. Natl. Acad. Sci. U. S. A.* **98**, 2312–2316
10. Chang, J. Y. (2004) *Biochemistry* **43**, 4522–4529
11. Creighton, T. E., Darby, N. J., and Kemmink, J. (1996) *FASEB J.* **10**, 110–118
12. Weissman, J. S., and Kim, P. S. (1991) *Science* **253**, 1386–1393
13. Chang, J. Y. (1996) *Biochemistry* **35**, 11702–11709
14. Venhudova, G., Canals, F., Querol, E., and Aviles, F. X. (2001) *J. Biol. Chem.* **276**, 11683–11690
15. Chang, J. Y., Li, L., and Lai, P. H. (2001) *J. Biol. Chem.* **276**, 4845–4852
16. Salamanca, S., Li, L., Vendrell, J., Aviles, F. X., and Chang, J. Y. (2003) *Biochemistry* **42**, 6754–6761
17. Arolas, J. L., Lorenzo, J., Rovira, A., Castella, J., Aviles, F. X., and Sommerhoff, C. P. (2005) *J. Biol. Chem.* **280**, 3441–3448
18. Marx, P. F. (2004) *Curr. Med. Chem.* **11**, 2335–2348
19. Arolas, J. L., Popowicz, G. M., Lorenzo, J., Sommerhoff, C. P., Huber, R., Aviles, F. X., and Holak, T. A. (2005) *J. Mol. Biol.* **350**, 489–498
20. Rees, D. C., and Lipscomb, W. N. (1982) *J. Mol. Biol.* **160**, 475–498
21. Reverter, D., Fernandez-Catalan, C., Baumgartner, R., Pfander, R., Huber, R., Bode, W., Vendrell, J., Holak, T. A., and Aviles, F. X. (2000) *Nat. Struct. Biol.* **7**, 322–328
22. Bieth, J. G. (1995) *Methods Enzymol.* **248**, 59–84
23. Reverter, D., Ventura, S., Villegas, V., Vendrell, J., and Aviles, F. X. (1998) *J. Biol. Chem.* **273**, 3535–3541
24. Arolas, J. L., Bronsoms, S., Lorenzo, J., Aviles, F. X., Chang, J. Y., and Ventura, S. (2004) *J. Biol. Chem.* **279**, 37261–37270
25. Chang, J. Y., Li, L., and Bulychev, A. (2000) *J. Biol. Chem.* **275**, 8287–8289
26. Chang, J. Y., Li, L., Canals, F., and Aviles, F. X. (2000) *J. Biol. Chem.* **275**, 14205–14211
27. Salamanca, S., Villegas, V., Vendrell, J., Li, L., Aviles, F. X., and Chang, J. Y. (2002) *J. Biol. Chem.* **277**, 17538–17543
28. Ellgaard, L., and Ruddock, L. W. (2005) *EMBO Rep.* **6**, 28–32
29. Hiniker, A., and Bardwell, J. C. (2004) *Trends Biochem. Sci.* **29**, 516–519
30. Shin, H. C., and Scheraga, H. A. (2000) *J. Mol. Biol.* **300**, 995–1003
31. van den Berg, B., Chung, E. W., Robinson, C. V., Mateo, P. L., and Dobson, C. M. (1999) *EMBO J.* **18**, 4794–4803
32. Bastolla, U., and Demetrius, L. (2005) *Protein Eng. Des. Sel.* **18**, 405–415
33. Wedemeyer, W. J., Welker, E., Narayan, M., and Scheraga, H. A. (2000) *Biochemistry* **39**, 4207–4216
34. Schymkowitz, J., Borg, J., Stricher, F., Nys, R., Rousseau, F., and Serrano, L. (2005) *Nucleic Acids Res.* **33**, (Web Server issue) W382–W388
35. Chang, J. Y., and Li, L. (2002) *FEBS Lett.* **511**, 73–78
36. Ventura, S., Vega, M. C., Lacroix, E., Angrand, I., Spagnolo, L., and Serrano, L. (2002) *Nat. Struct. Biol.* **9**, 485–493
37. Vendrell, J., Aviles, F. X., and Fricker, L. D. (2004) *Metalloproteinases in Handbook of Metalloproteins Vol. 3* (Messerschmidt, A., Bode, W., and Cygler, M., eds) pp. 176–189, John Wiley & Sons, Ltd., New York
38. Torres, A. M., and Kuchel, P. W. (2004) *Toxicon* **44**, 581–588
39. Barbosa Pereira, P. J., Segura-Martin, S., Oliva, B., Ferrer-Orta, C., Aviles, F. X., Coll, M., Gomis-Ruth, F. X., and Vendrell, J. (2002) *J. Mol. Biol.* **321**, 537–547
40. Bouma, B. N., and Meijers, J. C. (2003) *J. Thromb. Haemost.* **1**, 1566–1574
41. Eichinger, S., Schonauer, V., Weltermann, A., Minar, E., Bialonczyk, C., Hirschl, M., Schneider, B., Quehenberger, P., and Kyrle, P. A. (2004) *Blood* **103**, 3773–3776
42. Nagashima, M., Werner, M., Wang, M., Zhao, L., Light, D. R., Pagila, R., Morser, J., and Verhallen, P. (2000) *Thromb. Res.* **98**, 333–342
43. Walker, J. B., Hughes, B., James, I., Haddock, P., Kluff, C., and Bajzar, L. (2003) *J. Biol. Chem.* **278**, 8913–8921